Linking pore size and structure to the fatigue performance of sintered steels

Michael Andersson and Mats Larsson

Höganäs AB

Abstract

In this paper it is demonstrated how fine powder based materials can be used to improve fatigue strength. The increase in strength is accomplished by the smaller pores in the fine powder based materials. Also, a model linking pore size to fatigue strength is presented. This model is based on fracture mechanics in combination with an estimate of the largest pore sizes using extreme value statistics. Such a model can be used both to investigate the influence of different parameters on PM fatigue and to predict the fatigue strength of a material.

Introduction

The porosity of PM steels has a major influence on the fatigue properties of the materials since the pores act as natural initiation point for fatigue cracks. These typically start at the largest pores in a stressed area. This is particularly the case for hardened materials where the pores tend to be more influential than in softer materials. Thus, by reducing the sizes of the largest pores the fatigue strength of PM can be improved to meet the continuously increasing demand for higher performance.

Increasing density is often seen as the way to improve fatigue strength. But density is only a secondary parameter. Keeping all other parameters constant and increase density will lead to smaller pores, and thus improved fatigue strength. But if the pore size is reduced by some other means fatigue strength will also be increased, even if density is kept constant. One way to reduce pore sizes is to use finer powders. In this paper it will be demonstrated how fatigue properties can be improved by using finer powder.

Also, a model is presented showing the relationship between porosity and fatigue. By using extreme value statistics the expected size of the largest pore is calculated. A linear elastic fracture mechanics (LEFM) model is then used to link pore size to fatigue properties. This provides a sound physical interpretation of the results, which can be used both to understand the underlying fatigue properties of PM steels and to predict fatigue properties from analysis of microstructure and porosity.

In [2], the well known Murakami model, cf. [1], was applied to fatigue of soft PM steels and the relationship between fatigue and porosity investigated. The main difference between the model presented here and the Murakami model, which is also a LEFM model, is that here the fatigue threshold is treated as a constant. It has been suggested by Bergmark, cf. [3], that for soft PM materials the Murakami model is a valid approach but for hardened materials a standard LEFM model should be applied.

Materials

The materials used in this study was a pre-alloyed powder with 1.5% Mo as well as a diffusion alloyed powder with 2% Ni and 1% Mo diffusion bonded to a pure iron powder. To produce powders with different particle sizes the base powders were sieved to different sizes. FS-bars were compacted at 700 MPa with the tool die heated to 50°C to produce a sintered density of 7.2 g/cm^3.

The materials were sintered at 1120°C or 1250°C in 90/10 N_2/H_2 for 30 min. After sintering the specimens were case hardened with an austenization temperature of 920°C and 0.8% C-potential followed by quenching in oil. Finally the specimens were tempered at 180°C for 60 min in air. This procedure gave martensitic microstructures, for the diffusion alloyed materials some Ni-rich austenite was also present. A summary of the different materials is shown in Table 1, where d_{50} denotes the mean particle size for the different powders.

Table 1. Summary of materials in the investigation and the results from fatigue testing.

Material	Type	d_{50} [μm]	T_{sinter} [°C]	σ_{50} [MPa]	s [MPa]	σ_{90} [MPa]
A	pre-alloyed	103	1250	478	16	457
				487	45	424
B	pre-alloyed	103	1120	432	56	355
C	pre-alloyed	63	1250	534	11	518
D	pre-alloyed	52	1250	557	18	531
E	pre-alloyed	44	1250	578	21	549
				589	41	530
F	pre-alloyed	44	1120	543	45	481
G	pre-alloyed	34	1250	576	<7.5	566
H	diffusion alloyed	49	1250	553	19	526
I	diffusion alloyed	49	1120	522	25	487

Fatigue testing

Fatigue testing was done in displacement controlled, plane bending fatigue with a test frequency of 25-30 Hz and load ratio R = - 1. ISO 3928 fatigue test bars with a 5×5 mm^2 cross section were used. Before testing the corners of each specimen were carefully ground to remove burr from the compaction. Testing was done using the staircase method according to MPIF Standard 56 [4] and the run-out limit was set to $2 \cdot 10^6$ cycles. The tests were considered a failure and stopped if the compliance of the test bar was raised 2.5%. The endurance limit with 50% and 90% survival rate, σ_{50} and σ_{90} respectively, were calculated as well as the standard deviation. s. Each test series consisted of 25 specimens to ensure reliable results.

The resulting fatigue properties are presented in Table 1. As can be seen from the table fatigue properties are increased as the powder size decreases. Materials A and E were tested at two occasions and the results are consistent between the rounds except for the standard deviation which was higher during the second testing. The scatter for materials B and F are also somewhat higher than is normally expected. Since material A is the reference material the large scatter for some of the specimens is not related to the fine powder.

Pore size analysis

Fatigue cracks will start at the largest pore in the stressed area of the material. Thus to find a model for fatigue strength of PM materials the maximum pore area must be determined. Extreme value statistics is a powerful tool to quantify rare events and it has also been applied

to defects in materials, see for instance [1]. Here extreme value statistics is used to calculate the largest pore that can be expected in a volume of the material.

The Gumbel distribution, cf. [5], will be used for the largest pore distribution. This distribution will occur when taking the maximum of a series of values belonging to an exponential distribution and, as will be shown below, it fits the experimental data for pores in PM steels well. The Gumbel distribution function is given by:

$$F_0(x) = \exp\left[\exp\left(-\frac{x-\lambda}{\delta}\right)\right] \quad (1)$$

where λ and δ are parameters in the distribution. Now it should be noted that this distribution is linked to the size of the scanned volume when determining the parameters. Thus to calculate the maximum size in a different volume the distribution must be rescaled. By assuming that the number of pores in a part of the material is proportional to the volume the distribution of maximum pore area in a volume V can be determined by:

$$F(x) = [F_0(x)]^{\frac{V}{V_0}} = \exp\left[\frac{V}{V_0}\exp\left(-\frac{x-\lambda}{\delta}\right)\right] \quad (2)$$

where V_0 is the volume.

To determine λ and δ a method described for instance in [1] is used. A cross section of the material is divided into subareas, as shown in Figure 1. The cross section is taken in the plane with the highest normal stress since it is this area that will cause crack initiation. For each subsection the convex area of the largest pore is determined. These are then sorted from the smallest to the largest and numbered i=1..N, where N is the total number of subsections. The largest pore area of each subsection is denoted A_i. In this case N=55..80 subsections were scanned each with area A_0=0.25 mm^2.

Next a cumulative probability value is assigned to each measurement according to:

$$F_i = \frac{i}{N+1} \quad (3)$$

and the distribution function is rewritten as:

$$y(x) = -\ln\left[-\ln F(x)\right] = \frac{x-\lambda}{\delta} - \ln\frac{V}{V_0} \quad (4)$$

Remembering V=V_0 for the scanned volume this equation can be used to calculate λ and δ by a least squares regression between x_i=A_i and y_i=-ln[-ln F_i].

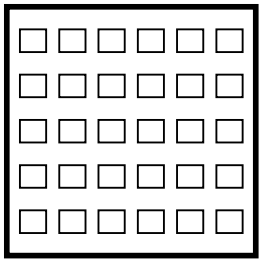

Figure 1. Illustration of the division of the specimen cross section into subsections for scanning.

Since the largest pore should be determined for a given volume the scanned area must be transformed into a volume. In [1] it is suggested that

$$V_0 = A_0 \cdot \frac{1}{N} \sum \sqrt{A_i} \qquad (5)$$

I.e. the depth of the volume is approximated as the average of the square root of the maximum pore areas. This is an empirical formula that has been proven useful and it will also be used here.

In Figure 2 the measured pore areas are plotted against y_i, the regression lines from the Gumbel distributions are also shown in the figure. It is clear that the Gumbel distribution fits well with the measured values. Some differences in the upper part of the distribution is seen but this is normal and due to uncertainties in the measured values here. For materials G-I it can also be seen that one point falls far outside the rest of the distribution having a very large area. These points were investigated by optical microscopy and found to be agglomerates. Thus they don't belong to the pore size distribution investigated and were excluded from the analysis.

Now, given the calculated values of λ, δ and V_0 the extreme value distribution for any volume V can be determined. In this case the distribution for the test specimens needs to be determined. Using the entire volume of the test specimens will overestimate the largest pore since the cross section will vary as well as the bending stresses. Sonsino [6] has suggested that the volume with stresses exceeding 90% of the maximum stress in the body should be used to evaluate fatigue strength. This model is also adopted here and the 90% volume of the ISO 3928 test bar in plane bending is estimated to 14.2 mm^3.

Rewriting equation (4) the maximum pore area with probability α can be written as:

$$A_{(\alpha)} = \lambda + \delta \left[\ln \frac{V}{V_0} - \ln\left(-\ln \alpha\right) \right] \qquad (6)$$

To calculate the 50% fatigue limit (σ_{50}) the median area is used and α = 0.50, and to calculate the fatigue limit with 90% survival (σ_{90}) α = 0.90 and so on.

Table 2. Gumbel distribution parameters and calculated pore areas.

Material	**d_{50} [μm]**	**λ [μm^2]**	**δ [μm^2]**	**V_0 [mm^3]**	**$A_{(50)}$ [μm^2]**	**$A_{(90)}$ [μm^2]**
A	103	769	225	0.230	1779	2203
B	103	835	303	0.275	2140	2711
C	63	623	165	0.181	1404	1714
D	52	514	105	0.144	1036	1235
E	44	426	89.4	0.119	885	1054
F	44	429	90.8	0.133	886	1057
G	34	336	81.8	0.0989	773	927
H	49	310	72.1	0.0995	694	830
I	49	298	81.9	0.104	731	885

The resulting parameters in the distribution are shown in Table 2 along with the predicted largest pore areas for the fatigue bars. It is clear that maximum pore area increased as the powder size increased. Thus, by using finer powders the largest pores will also shrink.

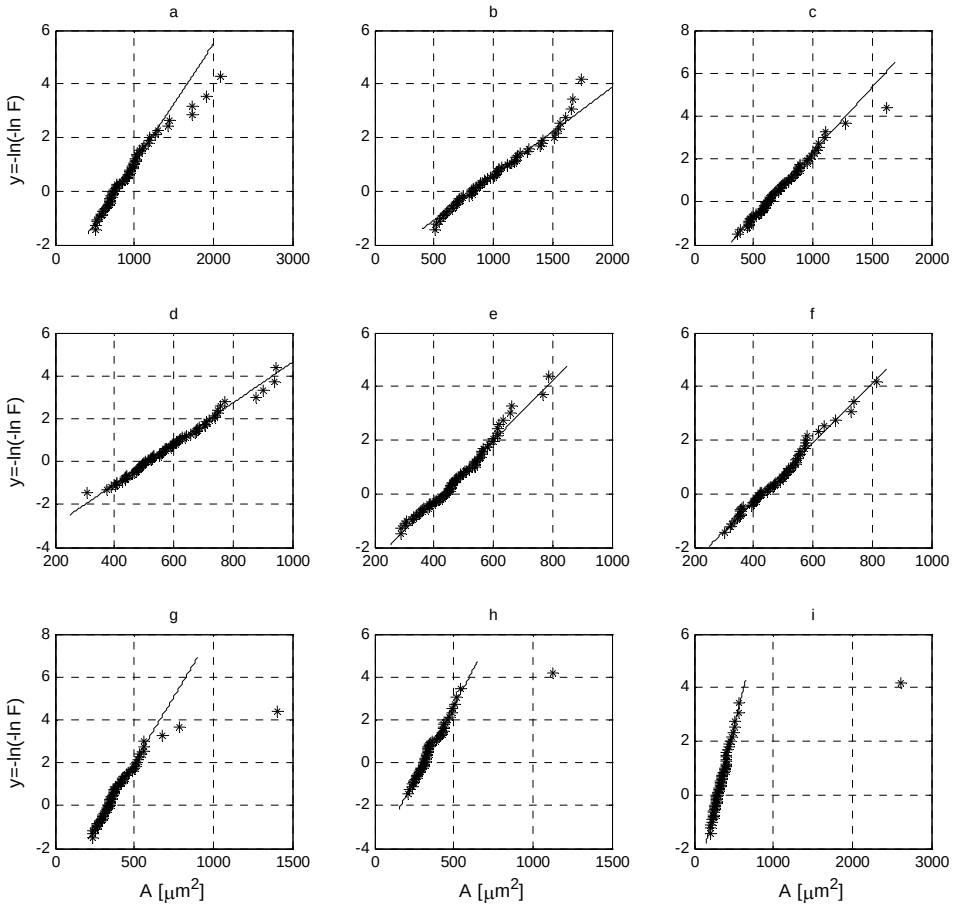

Figure 2. Measured extreme value distributions of the porosity, including the fitted Gumbel distributions.

Fatigue model

To link pore size with fatigue strength a fracture mechanics model is developed. By using fracture mechanics a physical interpretation between crack length and fatigue limit is established. In this paper the model is based on LEFM which is considered to be sufficient since the treated materials are martensitic. This means that the yield strength of the materials will be high leading to a small plastic zone ahead of the crack tip.

It is well established that fatigue crack growth does not occur when the stress intensity factor drops below a certain threshold value. By using a handbook formula for the stress intensity factor ΔK the equation for the fatigue limit can be written as:

$$\Delta K_{th} = \Delta K = \Delta\sigma_w \sqrt{\pi a} \cdot f \qquad (7)$$

where ΔK_{th} is the threshold for fatigue crack growth, $\Delta\sigma_w$ the stress range at the fatigue limit, a the length of the largest defects in the material and f a geometry factor. Since the fatigue cracks are assumed to start at the largest pores, crack length a should be replaced by pore size. From experience it is known that the cracks typically start at the corners of the fatigue bars. This is due to the fact that for a given crack area a corner crack will give a higher stress

intensity than an edge crack in another position. According to[7] $f = 0.722$ for a corner crack in the shape of a quarter circle.

Furthermore, Murakami [1] has shown that when calculating stress intensity factors the convex crack area can be used as a good approximation instead of crack length. Since convex crack area, or in this case pore area, is more easily measured experimentally than crack length it is convenient to work with area. For a quarter circle with radius a the area is:

$$A = \frac{\pi a^2}{4} \tag{8}$$

Combining this equation with the above equation for crack initiation the fatigue limit can be expressed as:

$$\sigma_w = \frac{\Delta K_{th}}{1{,}36 \cdot A^{\frac{1}{4}}} \tag{9}$$

Murakami [1] has suggested that the threshold value depends on defect size through the relationship:

$$\Delta K_{th} = 3.3 \cdot 10^{-3} \cdot \left(HV + 120\right) \cdot A^{\frac{1}{6}} \tag{10}$$

where HV is the Vickers hardness and A defect area. This means that the threshold will change with defect size. Combining this equation with an expression for the stress intensity factor leads to the well known Murakami model for fatigue. However, in [3] it was suggested that there is a transition region between the Murakami model and a fracture mechanics model with constant ΔK_{th}. For hard materials, such as the ones in this study the transition can be expected to be below the pore sizes found in the materials. Thus it is motivated to treat ΔK_{th} as a constant. That means that the fatigue limit is expected to be proportional to $\sigma_w \sim A^{-1/4}$, compared to the $\sigma_w \sim A^{-1/12}$ relationship in the Murakami model [1]. This is consistent with the fact that harder materials are known to be more sensitive to large pores than softer ones.

In Figure 3 the measured fatigue limits are plotted against calculated maximum pore areas, ±10% scatter lines have also been plotted. The vertical bars show 95% confidence intervals for σ_{50}. In the figure a regression line based on equation (9) has also be plotted, where ΔK_{th} was fitted by a least square regression to the experimental data. As can be seen the $\sigma_w \sim A^{-1/4}$ model fits the experimental data very well. The exception is the diffusion alloyed materials which have a fatigue limit that is somewhat lower than the others with a comparable pore size. This is most likely due to soft nickel rich austenite present in the microstructures of these materials.

The calculated threshold was found to be $\Delta K_{th} = 4.2$ MPa√m. In [8] Yu and Topper found ΔK_{th} for martensitic microstructures to be in the range 3.4 to 4.6 MPa√m. Thus the measured threshold is well in the range of what can be expected for these materials.

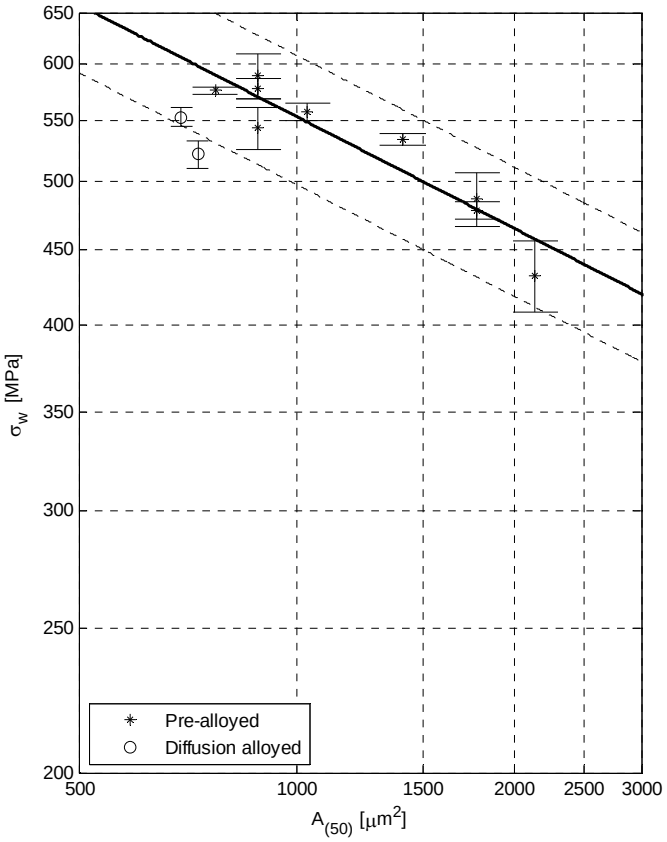

Figure 3. Measured fatigue limits plotted against largest pore areas.

Summary and discussion

The close relationship between the size of the largest pores and the fatigue strength of PM steels has been demonstrated. By reducing the size of the largest pores pronounced increase in fatigue strength was achieved. In this case the reduction in pore sizes was achieved by using finer powder particles.

To quantify the influence of porosity extreme value statistics in combination of optical microscopy has proven useful. By using extreme value distributions rare events, such as the occurrence of large pores, can be predicted. In this paper it was assumed that the maximum pore size follows a Gumbel distribution. This choice is motivated by the good fit to the measured data, as seen in Figure 2. But it may be interesting to explore other extreme value distributions as well. Also, some points were found that belonged to a secondary defect distribution, in this case agglomerates. In this case these secondary defects were rare enough not to influence the fatigue strength but in general all defect distributions need to be investigated to determine the largest initiation size.

Furthermore it would be of interest to quantify the accuracy of the prediction of the largest pore size. This could be done both through a theoretical investigation of the statistical prediction and through fractography. By making a fractographic investigation of broken fatigue specimens the actual initiation areas can be measured and compared to the predicted areas.

Another point that should be further explored is the somewhat lower performance of the diffusion alloyed materials compared to the pre-alloyed materials. This difference is expected to be due to the presence of nickel rich austenite in the microstructure of the diffusion alloyed

materials. The austenite phase is soft allowing for fatigue cracks to easily nucleate here. It is well known that in diffusion alloyed materials cracks sometimes initiate outside of pores [9]. In these cases the interaction between pores and softer phases is important. One way to handle such interactions would be to include some of the soft phase as a virtual crack extension. For the Ni rich austenite in the diffusion alloyed materials this would mean that the data points in Figure 3 were moved a few hundred square microns to the right, thus moving them close to the prediction line.

Finally, by having a physically founded model, for instance linking pore size to fatigue life through fracture mechanics allows for investigations of how different parameters influence fatigue of PM steels. The model proposed here is based on LEFM and works well for hardened materials. For softer materials the use of non linear fracture mechanics may be a suitable route. Also, such a model can be used to predict fatigue behaviour of various materials, potentially even taking variations in stress and pore distributions into account. However, the model is still under development and further investigations of the influence of factors such as residual stresses and secondary phases in the microstructure must be performed. Also, the methods associated with the extreme value analysis of the porosity must be further examined and the uncertainties in the estimates determined.

Conclusions

A large improvement in fatigue strength of PM steel was found by using smaller powder particles. Furthermore it was demonstrated that the increase in fatigue strength was the result of a reduction in pore sizes. To estimate the size of the largest pores extreme value statistics was found to be a useful tool. Also, by combining the pore size analysis with a fracture mechanics model the fatigue strength of the material was linked to porosity and a prediction model for fatigue strength derived.

References

[1]. Murakami Y., *Metal Fatigue: Effects of Small Defects and Nonmetallic Inclusions*, Elsevier, 2002

[2]. Beiss P. and Lindlohr S., *Porosity Statistics and Fatigue Strength of Sintered Iron*, International Journal of Powder Metallurgy, vol. 45, Issue 2, 2009

[3]. Bergmark A., *Influence of Maximum Pore Size on the Fatigue Performance of PM Steel*, Proceedings of the International Conference DF PM 2005, editors Parilák L. and Danninger H., Stará Lesná, 2005

[4]. MPIF Standard 56, MPIF, 2001

[5]. Gumbel E.J., *Statistics of Extremes*, republication of the 1958 Columbia University Press edition, Dover Publications, 2004

[6]. Sonsino C.M., *Zur Bewertung des Schwingfestigkeitsverhaltens von Bauteilen mit Hilfe örtlicher Beanspruchungen*, Konstruktion, vol. 45, pp. 25-33, 1993

[7]. Anderson T.L., *Fracture Mechanics, Fundamentals and Applications*, 2nd edition, CRC Press, 1995

[8]. Yu M.T. and Topper T.H., *Effect of carbon content and microstructure on near threshold crack propagation*, Int. J. Fatigue, vol 11, No 5, pp. 335-340, 1989

[9]. Bergmark A. and Alzati L., *Fatigue crack walk in Cu-Ni-Mo alloyed PM steel*, Fatigue and Fracture of Engineering Materials and Structures, vol. 28, No. 1-2, 2005